FACILITY FORM 602
N65-33280 (ACCESSION NUMBER)
(THRU)
20 (PAGES)
1 (CODE)
CR 64809 (NASA CR OR TMX OR AD NUMBER)
02 (CATEGORY)

PARAMETER DEPENDENCE OF PHASE AND LOG AMPLITUDE SCINTILLATION

by

J. F. Phelan and K. C. Yeh

GPO PRICE $ ________
CSFTI PRICE(S) $ ________
Hard copy (HC) 1.00
Microfiche (MF) .50
ff 653 July 65

NsG 24-59

June 30, 1965

Sponsored by:

National Aeronautics and Space Administration

Washington 25, D. C.

Electrical Engineering Research Laboratory
Engineering Experiment Station
University of Illinois

Urbana, Illinois

Parameter Dependence of Phase and Log Amplitude Scintillation

Abstract:

33280

By means of numerical computation based on the equations developed by Yeh [1962] for phase and log amplitude correlation of waves transmitted through a slab of random irregularities, the effects of variations in transmitter height, slab thickness, slab height and irregularity size are studied. A selected number of curves illustrating the effects of changes in these parameters are drawn. Using these curves as a basis, it is shown that, from experimental data, bounds may be established for some of these parameters.

Author

Introduction

Studies of wave propagation through a random medium are complicated by the presence of a large number of parameters. The basic formulation of the problem for the case of weak irregularities has been summarized in books by Chernov [1961] and Tatarski [1961]. However, difficulties arise when specific values and the dependence of these values with respect to certain parameters are desired. This is especially true if irregularities are anisotropic, as usually is the case in experimental investigations. Therefore, it is desirable to compute numerically the phase departure and the logarithmic amplitude departure. The numerical values used are those found in the ionosphere work of studying scintillation of satellite radio signals. These results are presented graphically in this report.

The specific problem of interest is the signal statistics of a spherical wave emitted by a transmitter through an intervening slab of irregularities. This problem has been studied by a number of authors [Budden, 1965; deWolf, 1965; Komissarov, 1964; Yeh, 1962; Yoneyama, 1964; Yoneyama and Mushiake, 1965]. As far as possible the notations used here will follow those in the earlier paper [Yeh, 1962] except that the distances will not be normalized. The geometry of the problem is illustrated by Fig. 1 where the distances a, b, c, and z are shown clearly. Other parameters are the three-dimensional "sizes" of irregularities ℓ_x, ℓ_y and ℓ_z. The mean square values of the phase departure and the logarithmic amplitude departure are obtained by numerically integrating (30) which is then substituted into the equations (41) and (42) of Yeh [1962].

Presentation of Graphs

Figs. 2 and 3 show the effect on phase and log amplitude departure, respectively, caused by variations in slab thickness, slab height, transmitter height, and transmitter location above the slab. Each set of curves assumes $\ell_x = 1.0$ km and a value of ℓ_y from .25 km to 32 km. The curves of a set are grouped by the value of b, the slab thickness. The individual curves represent departure vs. transmitter height, z, for a given transmitter location above the slab, a. The actual value of the departure is dependent upon ℓ_z as well as $\langle\mu^2\rangle \langle\epsilon^2\rangle$. The frequency chosen for the graphs is 19.1 Mc/s.

It is immediately apparent that, for small values of ℓ_y, the layer thickness b has the predominant effect on both phase and amplitude departure. The transmitter location above the slab, a, appears to be the major secondary factor. Moving from left to right, in Figure 2 we see that as ℓ_y increases, thephase departure markedly increases until ℓ_y is about 4 km; but in contrast, as shown in Figure 3, the amplitude departure markedly decreases as ℓ_y increases until ℓ_y reaches a "critical" value, in this case, approximately 8 km. For values of ℓ_y larger than the "critical" values, changes in ℓ_y appear to have little effect on either the phase or amplitude departure.

Fig. 2 also shows that for small b the phase departure is nearly independent of ℓ_y and weakly dependent on a. However, for larger values of b the dependency on a becomes increasingly stronger as either b or ℓ_y is increased provided that ℓ_y is less than its "critical" value. For large values of ℓ_y, the set of curves differ little as ℓ_y is increased. This shows that if irregularities are extremely anisotropic the phase scintillation is more dependent on other parameters than ℓ_y.

In contrast, the amplitude departure shown in Fig. 3 decreases markedly with increasing ℓ_y even for small values of slab thickness, b. However, we again find that the dependency of amplitude departure on a becomes increasingly stronger as both b and ℓ_y increase, provided that ℓ_y is less than about 8 km, which appears to be a "critical" value. In addition, a similar dependency is shown with respect to transmitter height, z. As before, when ℓ_y is greater than the "critical" value the sets of curves look very similar.

Studying the interdependence of these parameters gives rise to the question of whether minimal "critical" values for ℓ_y existed and their dependency on ℓ_x. For this reason, as well as a general interest in the effect of the relationship of the ratio of ℓ_y to ℓ_x on phase and amplitude departure, Figs. 4 and 5 were constructed.

The curves in these figures are plots of phase and amplitude departure vs. ℓ_y with a, b and ℓ_x as parameters. Each set represents a given value of ℓ_x and, as with Figs. 2 and 3, the curves in each set are grouped by the value of slab thickness b. The curves in Fig. 4 are subgrouped by the transmitter height z.

In constructing Fig. 4, it was found to be impossible to draw meaningful curves which included more than one transmitter height z. The latter's effect on the log phase departure was greatly exceeded by the effect of variations in a. Furthermore, the sets of curves for a given value of b for various values of a were very similar for a wide range of choices of z. The fixed z = 12,800 km was therefore selected solely on the basis of graphic presentability.

The curves in both Figs. 4 and 5 appear to verify the existence of lower "critical" values for ℓ_y for all values of ℓ_x. They can be estimated to be in the neighborhood of .25 km except for very small values of b. Again, for all ratios of ℓ_x to ℓ_y, we find that the major factor affecting the phase and log amplitude departures, as might be expected, is the slab thickness b. Additionally, we note that the phase departure increases fairly rapidly with increases in either ℓ_x or ℓ_y if they are less than some "critical" value, which, for the most part, apparently lies in the neighborhood of 4 km to 8 km.

Perhaps the most striking result is the effect of irregularity size on log amplitude departure as shown by Fig. 5. The graphs for $\ell_x = 4$ km and $\ell_x = 16$ km show marked drops as ℓ_y increases.

In an effort to exploit the contrasting effect of slab thickness b on the phase and log amplitude departure, we computed the curves in Figs. 6, 7 and 8. A transmitter height z of 1200 km was chosen to correspond to the then probable height of the satellite S-66. The integrals were changed to permit the use of a mean layer height h rather than the distance c, as shown in the insert of Fig. 6. The latest experimental evidence seems to indicate that h = 350 km is a reasonable figure [McClure, 1964]. Random checks of plots for other values of h verified that this height yielded representative curves. Note that the new normalization makes the phase and log amplitude departure scales independent of frequency. It is hoped that these curves might lead to realizable experimental techniques for at least gross estimation of these parameters.

Fig. 6 is a plot of phase vs. amplitude departure for various values of ℓ_x. For all curves in this set f = 20 mc and $\ell_x = \ell_y$. The plot makes use of the important property

$$\langle Q^2 \rangle + \langle S^2 \rangle = Kb/f^2 \qquad (1)$$

where

$$K = 4 \langle \epsilon^2 \rangle \langle \mu_0^2 \rangle \pi^{5/2} \ell_z / c^2$$

Thus the curves superimposed for constant b are arcs of circles with a center at the origin.

The sets of curves in Fig. 6 have at least three characteristics which may be exploited. First, since

$$\langle S^2 \rangle / \langle Q^2 \rangle \leq 1 \tag{2}$$

we obtain, when (2) is substituted into (1),

$$Kb/f^2 \geq \langle Q^2 \rangle \geq Kb/2f^2 \text{ and } \langle S^2 \rangle \leq Kb/2f^2 \tag{3}$$

The relation (3) establishes the upper and lower bounds for phase scintillation, and the upper bound for amplitude scintillation.

Second, a line through the origin having slope $\langle S^2 \rangle / \langle Q^2 \rangle$ intersects $\langle Q^2 \rangle$ at a distance Kb/f^2 from the origin. Thus if b can be determined independently or estimated, we may find the normalized phase and amplitude departures which in turn yield the values of $\langle \epsilon^2 \rangle \langle \mu_0^2 \rangle \ell_z$. The factors $\langle \epsilon^2 \rangle$, $\langle \mu_0^2 \rangle$, and ℓ_z cannot be separated.

Third, for a fixed ratio of $\langle S^2 \rangle / \langle Q^2 \rangle$, ℓ_x changes very slowly as the slab thickness b is increased. In fact, for b less than about 300 km, the curves for constant ℓ_x are almost straight lines through the origin. It may be verified easily that the scaling factor for b is inversely proportional to the frequency (e.g. for 40 Mc/s signals, the slab thickness is b/2 as shown in Fig. 6). Thus, if the curve for a given ℓ_x is independent of frequency, we must have

$$\frac{\langle Q^2 \rangle_{20\ mc}}{\langle Q^2 \rangle_{40\ mc}} = \frac{\langle S^2 \rangle_{20\ mc}}{\langle S^2 \rangle_{40\ mc}} = 2$$

where $\langle Q^2 \rangle_{40\ mc}$ and $\langle S^2 \rangle_{40\ mc}$ are read from Fig. 6 by assuming b/2 is the slab thickness. If the curve is not independent of frequency then

$$\langle Q^2 \rangle_{20\ mc} - 2 \langle Q^2 \rangle_{40\ mc} = \delta$$

and the stronger the frequency dependency the larger the value of δ. We illustrate this graphically as follows.

For simplicity, let $\ell_x = \ell_y$. If the phase departure at 20 mc has a value q_1 and $\ell_x = \ell_{x_1}$, as shown in Fig. 7, then $b = b_1'$ and the phase departure at 40 mc should intersect the curve $\ell_x = \ell_{x_1}$ at $b_2' = b_1'/2$, i.e. $q_2 = q_1/2$.

If for the same phase departure at 20 mc, $\ell_x = \ell_{x_2}$, then $b = b_1$ and the phase departure at 40 mc should have the value $q_3 > q_1/2$ determined by the arc $b = b_2 = b_1/2$ and the curve for $\ell_x = \ell_{x_2}$, f = 40 mc.

By using separate phase and amplitude departure scales for each frequency (ratio f_1/f_2), and thus the same scale for b, we can reduce Fig. 7 to Fig. 8.

The curves in Fig. 9 were computed to study frequency dependence. In order to compare easily the change in departure due to frequency shift, frequency was eliminated as a scaling factor for b as illustrated above.

It will be noted that for values of ℓ_x such that 1 km $\leq \ell_x \leq$ 3.0 km, the frequency dependence is sufficiently strong to be verified experimentally. This is just the range of irregularities observed in the ionosphere work.

The question therefore arose as to whether this non-linearity existed in this range when $\ell_x \neq \ell_y$ and the curves in Fig. 10 were computed to examine the spacings for $\ell_y = 5\ \ell_x$, $\ell_y = 10\ \ell_x$, and $\ell_y = 15\ \ell_x$. The latter two sets of curves were identical within the plotting accuracy and $\ell_y = 15\ \ell_x$ was therefore omitted.

It is immediately apparent that the range of non-linearity includes $1.0 \text{ km} \leq \ell_x \leq 3.0 \text{ km}$. Further, it is also noted that for $\ell_x \geq 2.6 \text{ km}$, the two sets of curves are almost indistinguishable indicating that the anisotropic effect is unimportant in this region, a property also shown clearly in Figs. 4 and 5.

Conclusions

The study of ionospheric irregularities based upon measurement by a single receiver of the scintillation of radio signals from a satellite, even when supplemented by other information such as layer height and layer thickness, is plagued not only by the inherent difficulties of accurately measuring the scintillation itself, but also by the fact that there are a large number of combinations of parameters which would cause the same scintillation. However, it would appear that accurate measurement of both phase departure and amplitude departure coupled with measurements of layer height and thickness could do much toward establishing bounds for certain parameters and for some confirmation of theoretical results.

References

1. Budden, K. G., The Amplitude Fluctuations of the Radio Wave Scattered from a Thick Ionospheric Layer with Weak Irregularities, J. Atmosph. Terr. Phys. 27, 155-172, Feb. 1965.

2. Chernov, L. A., Wave Propagation in a Random Medium, English translation by R. A. Silverman (McGraw-Hill Book Co., Inc., New York, 1961).

3. deWolf, D. A., Point-to-Point Wave Propagation Through an Intermediate Layer of Random Anisotropic Irregularities: Phase and Amplitude Correlation Functions, IEEE Transactions on Antennas and Propagation AP-13, 48-51, Jan. 1965.

4. Komissarov, V. M., Amplitude and Phase Fluctuations and Their Correlation in the Propagation of Waves in a Medium with Random, Statistically Anisotropic Inhomogeneities, Soviet Physics-Acoustics 10, No. 2, 143, Oct.-Dec. 1964.

5. McClure, J. P., The Height of Scintillation-Producing Ionospheric Irregularities in Temperate Latitudes, J. Geophys. Res. 69, 2775-2780, 1964.

6. Tatarski, V. I., Wave Propagation in a Turbulent Medium, English translation by R. A. Silverman (McGraw-Hill Book Co., Inc., New York 1961).

7. Yeh, K. C., Propagation of Spherical Waves through an Ionosphere Containing Anisotropic Irregularities, J. Research of NBS, 66D, 621-636, 1962.

8. Yoneyama, T., Line-of-Sight Propagation in a Statistically Anisotropic Random Medium, ICMCI Summaries of Papers Part 1 Microwaves, Tokyo, 325, 1964.

9. Yoneyama, T. and Y. Mushiake, Scintillation Fading in Line-of-Sight Propagation Through a Statistically Anisotropic Turbulent Medium, IEEE Transactions on Antennas and Propagation, AP-13, 476-477, May 1965.

Figures

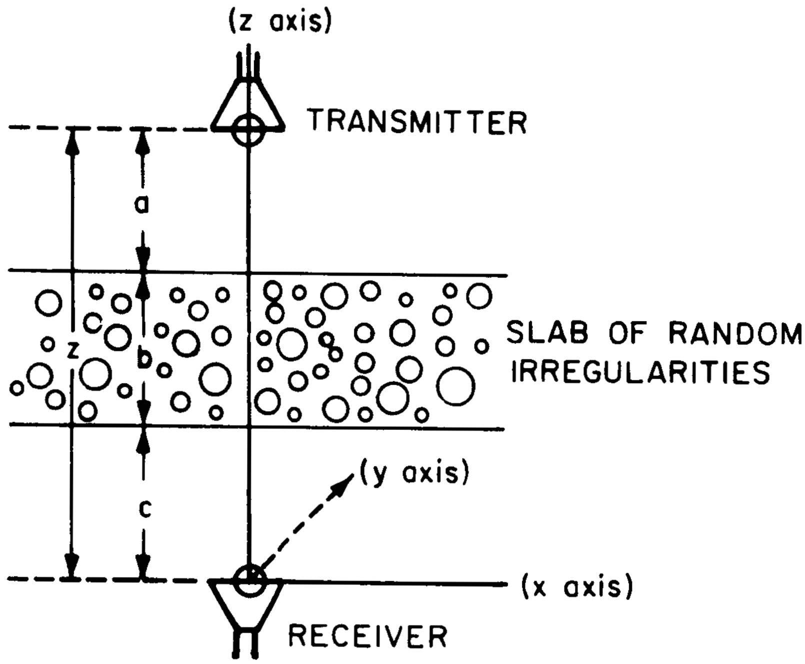
(z axis)
TRANSMITTER
a
z
b
c
SLAB OF RANDOM IRREGULARITIES
(y axis)
(x axis)
RECEIVER

FIGURE 1.

FIGURE 2

NORMALIZED

ROOT MEAN SQUARE VALUE PHASE DEPARTURE

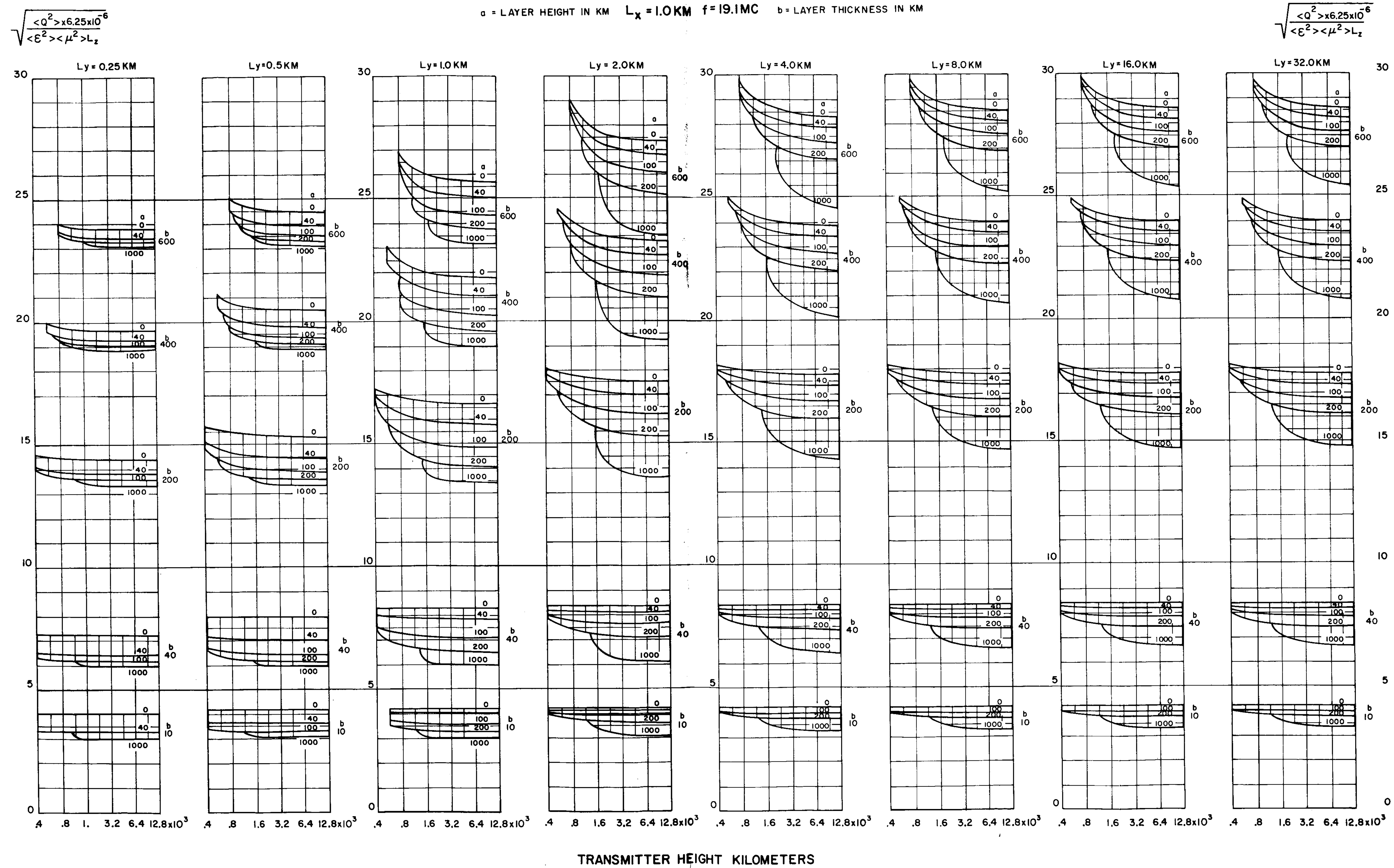

FIGURE 3

NORMALIZED ROOT MEAN SQUARE VALUE LOG AMPLITUDE DEPARTURE

a = LAYER HEIGHT IN KM $L_x = 1.0$ KM f = 19.1 MC b = LAYER THICKNESS IN KM

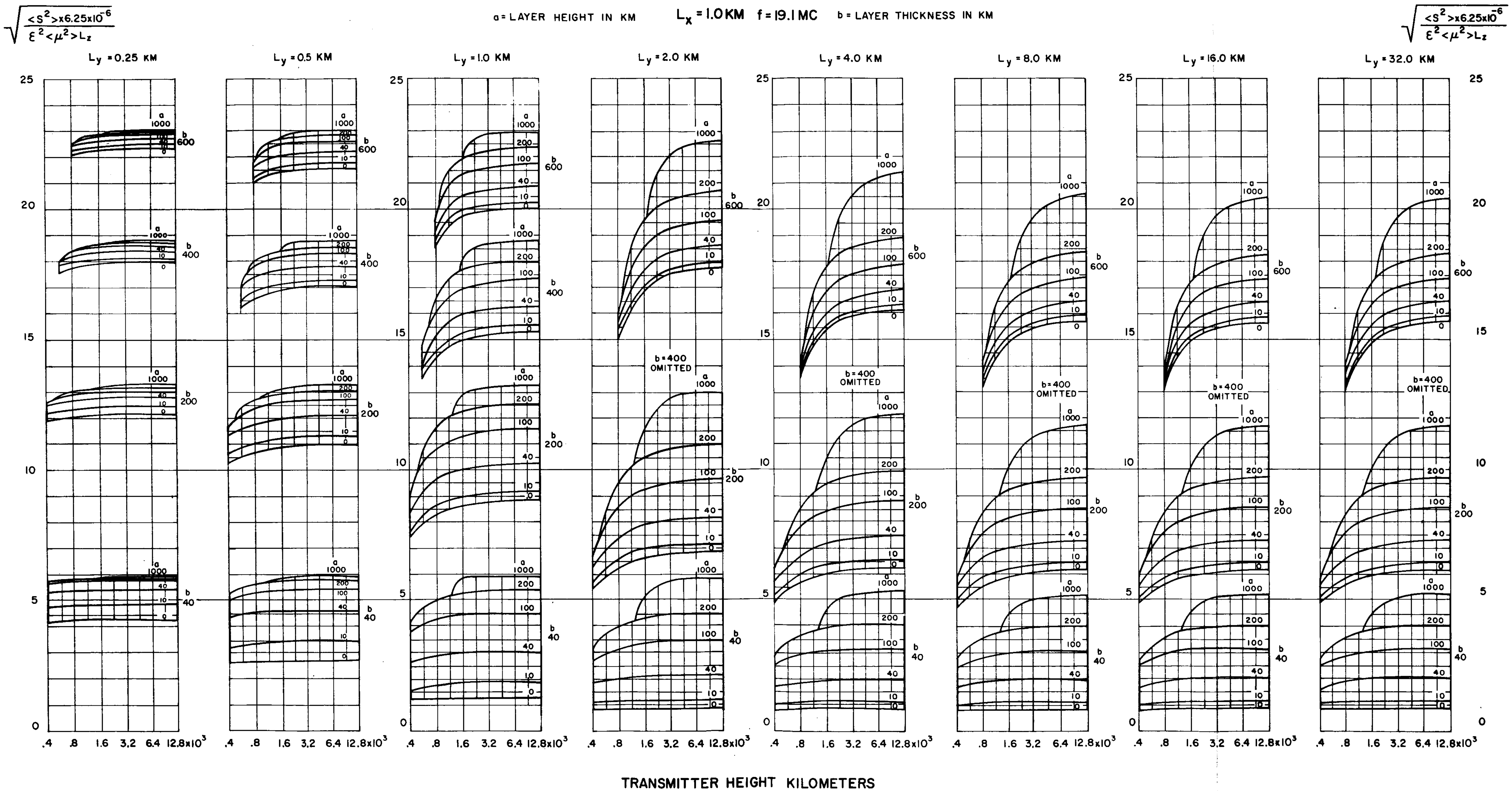

NORMALIZED ROOT MEAN SQUARE VALUE PHASE DEPARTURE

f = 19.1 MC

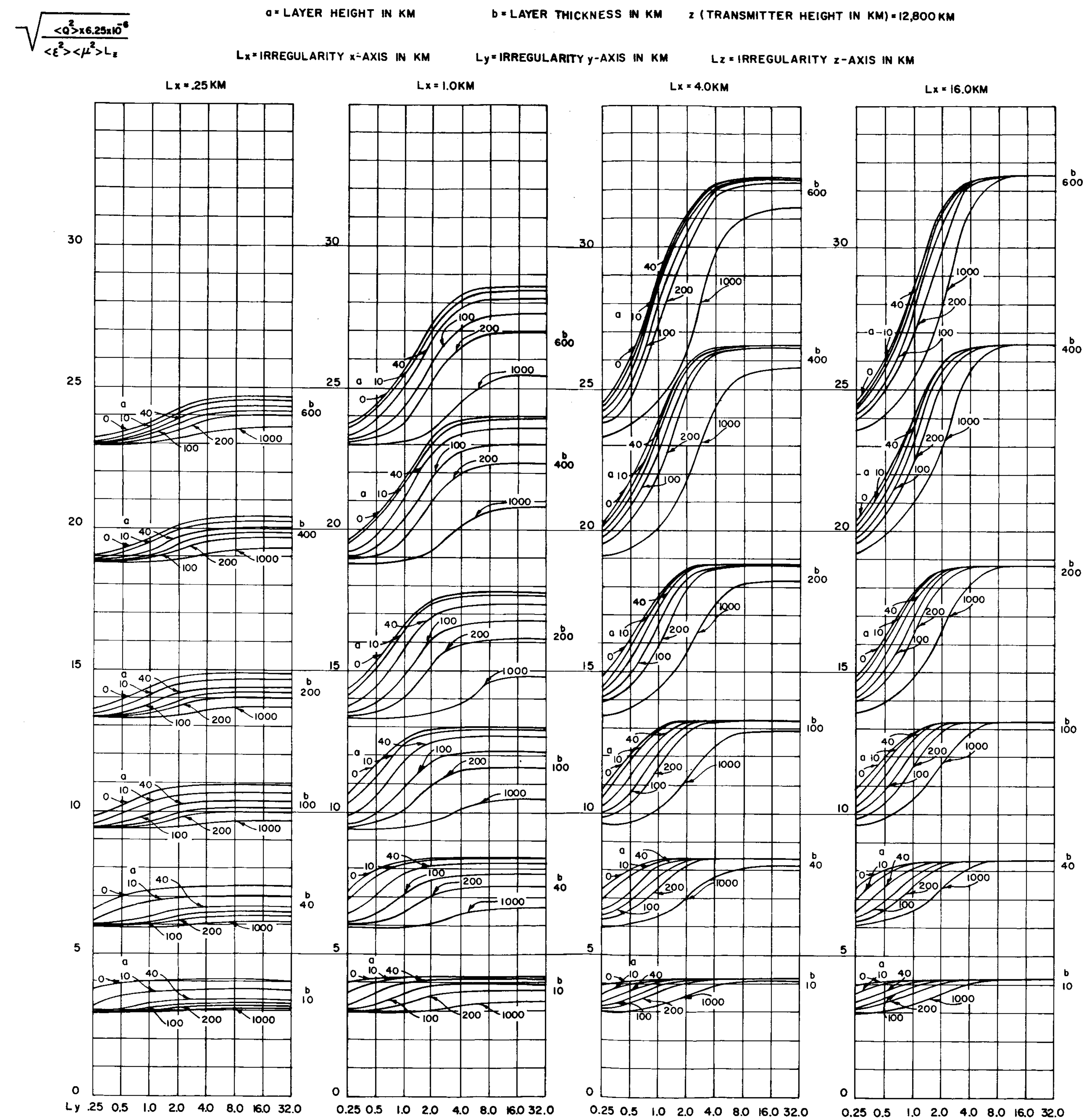

FIGURE 4.

NORMALIZED

ROOT MEAN SQUARE VALUE LOG AMPLITUDE DEPARTURE

f = 19.1 MC

a = LAYER HEIGHT IN KM b = LAYER THICKNESS IN KM z = TRANSMITTER HEIGHT IN KM

L_x = IRREGULARITY x-AXIS IN KM L_z = IRREGULARITY z-AXIS IN KM L_y = IRREGULARITY y-AXIS IN KM

$\sqrt{\dfrac{\langle S^2\rangle \times 6.25\times 10^{-6}}{\langle \varepsilon^2\rangle\langle \mu^2\rangle L_z}}$

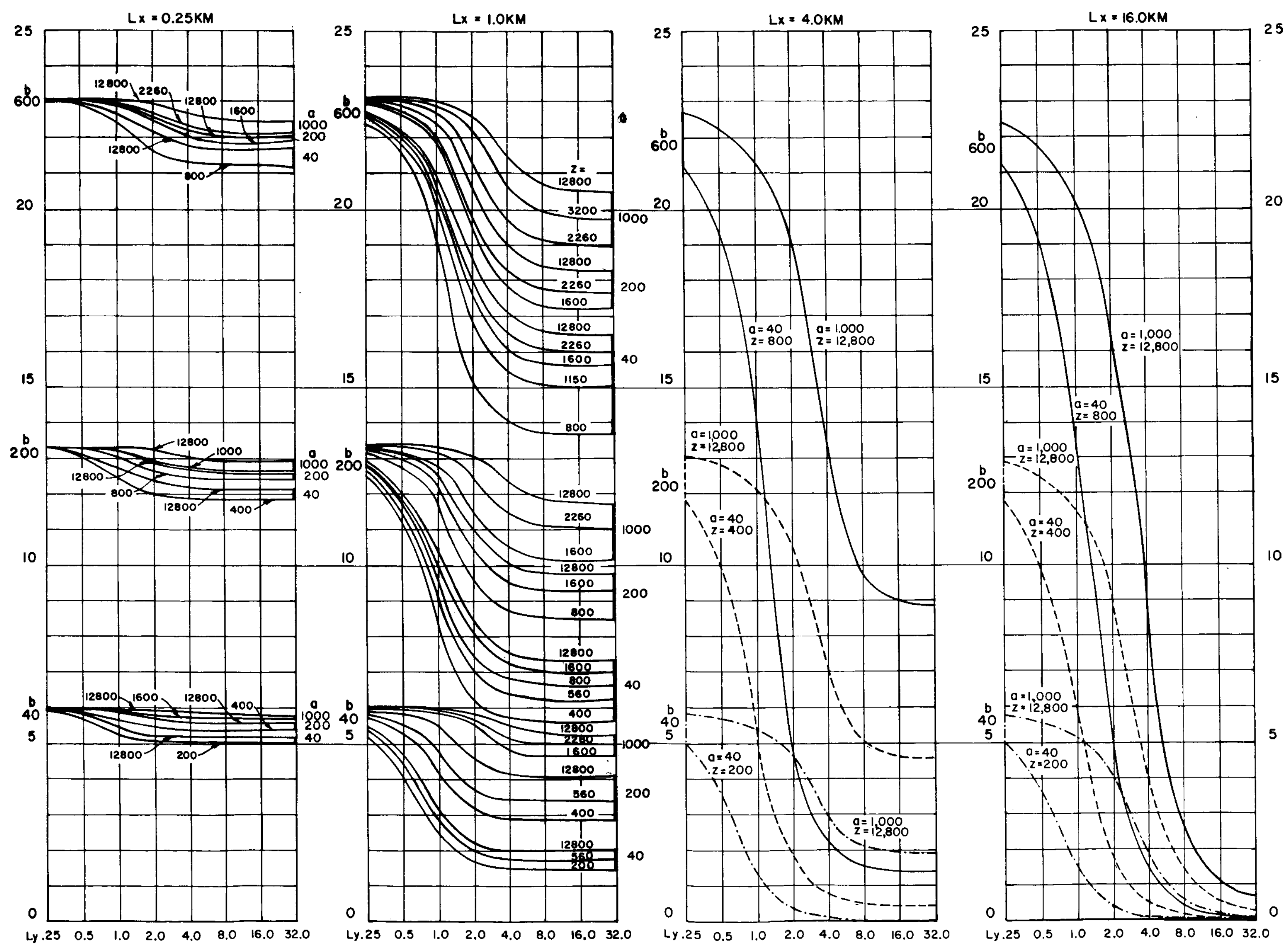

FIGURE 5.

FIGURE 6
RMS PHASE DEPARTURE vs. LOG AMPLITUDE FOR VARIOUS LAYER THICKNESSES

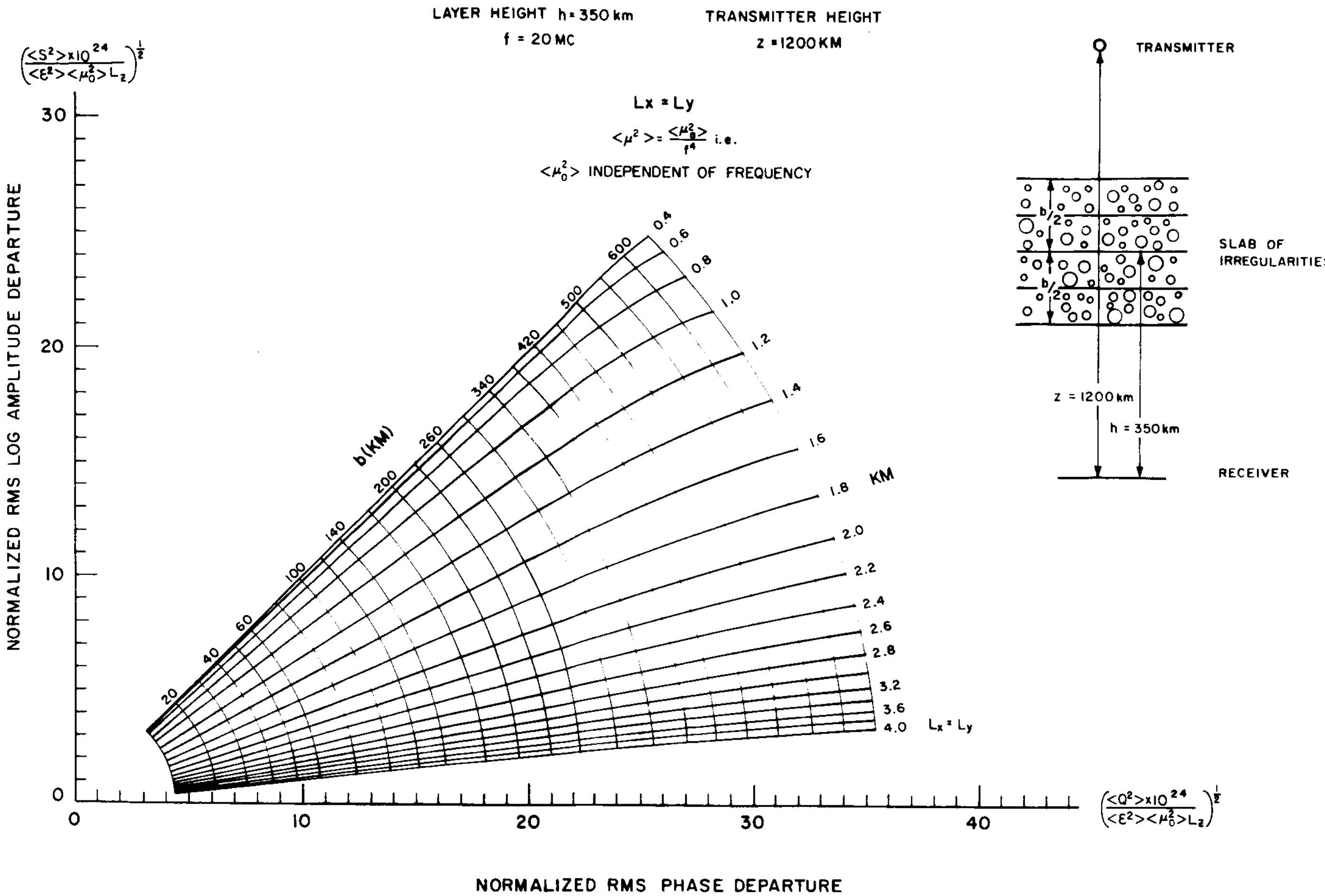

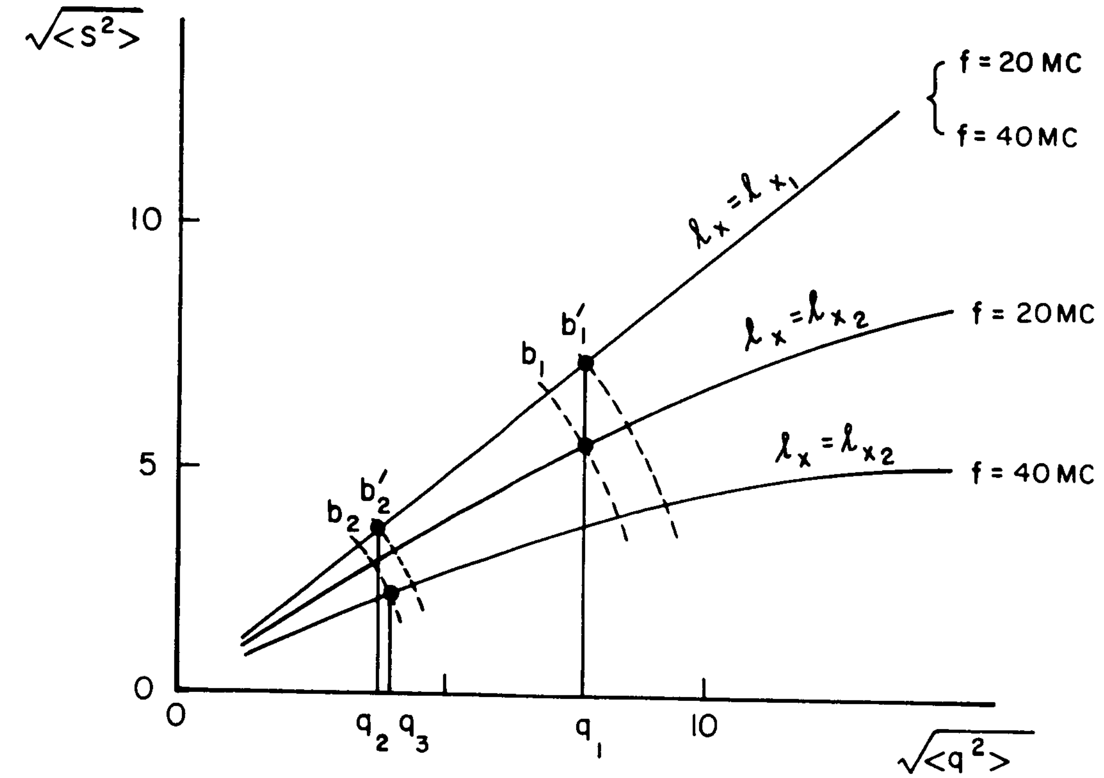

Figure 7.

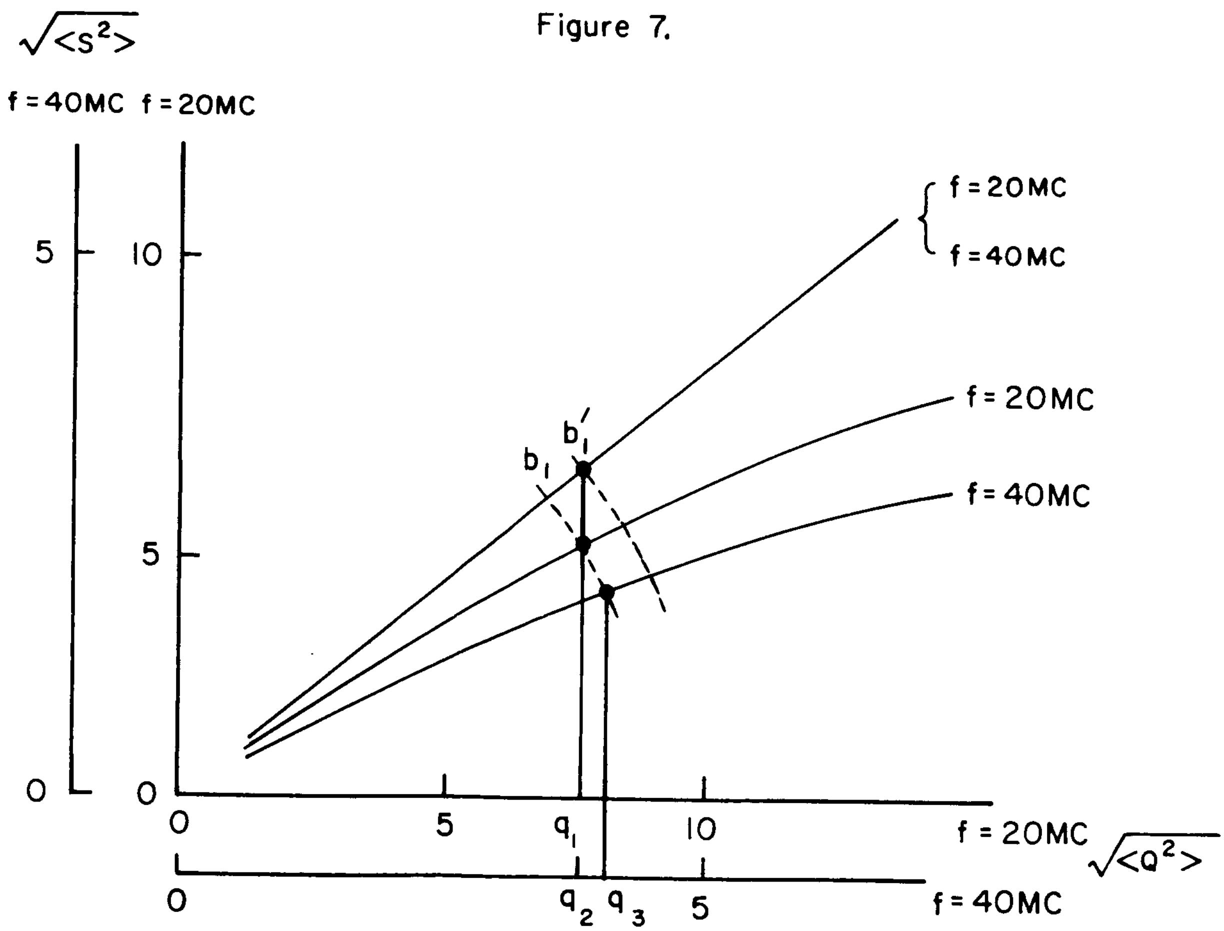

Figure 8.

FIGURE 9
EFFECT OF FREQUENCY ON PHASE DEPARTURE
AND LOG AMPLITUDE

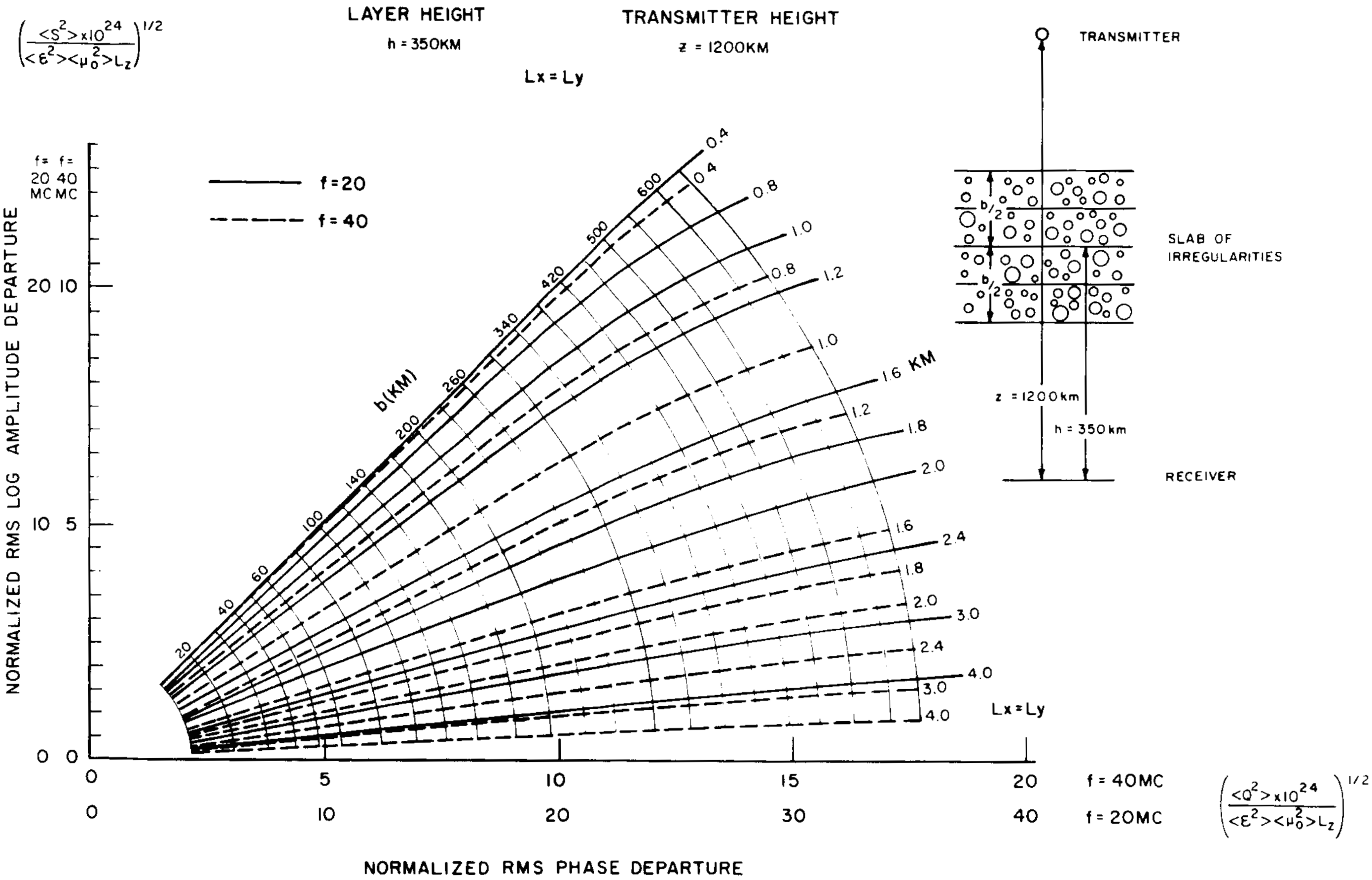

FIGURE 10
EFFECT OF RATIO Ly/Lx ON PHASE DEPARTURE AND LOG AMPLITUDE